Cytokine xxx (2015) xxx–xxx

Contents lists available at ScienceDirect

Cytokine

journal homepage: www.journals.elsevier.com/cytokine

P2X$_7$R activation drives distinct IL-1 responses in dendritic cells compared to macrophages

Pavlos C. Englezou [a], Simon W. Rothwell [a], Joseph S. Ainscough [a], David Brough [a], Robert Landsiedel [b], Alexei Verkhratsky [a], Ian Kimber [a], Rebecca J. Dearman [a,*]

[a] Faculty of Life Sciences, Smith Building, The University of Manchester, UK
[b] BASF SE, Experimental Toxicology and Ecology, Ludwigshafen, Germany

ARTICLE INFO

Article history:
Received 19 December 2014
Received in revised form 12 May 2015
Accepted 19 May 2015
Available online xxxx

Keywords:
Interleukin-1
P2X$_7$R
Dendritic cells
Macrophages
A-740003

ABSTRACT

The P2X$_7$R is a functionally distinct member of the P2X family of non-selective cation channels associated with rapid activation of the inflammasome complex and signalling interleukin (IL)-1β release in macrophages. The main focus of this investigation was to compare P2X$_7$R-driven IL-1 production by primary murine bone marrow derived dendritic cells (BMDC) and macrophages (BMM). P2X$_7$R expression in murine BMDC and BMM at both transcriptional (P2X$_7$A variant) and protein levels was demonstrated. Priming with lipopolysaccharide (LPS) and receptor activation with adenosine triphosphate (ATP) resulted in markedly enhanced IL-1 (α and β) secretion in BMDC compared with BMM. In both cell types IL-1 production was profoundly inhibited with a P2X$_7$R-specific inhibitor (A-740003) demonstrating that this release is predominantly a P2X$_7$R-dependent process. These data also suggest that P2X$_7$R and caspase-1 activation drive IL-1α release from BMDC. Both cell types expressed constitutively the gain-of-function P2X$_7$K as well as the full P2X$_7$A variant at equivalent levels. LPS priming reduced significantly levels of P2X$_7$A but not P2X$_7$K transcripts in both BMDC and BMM. P2X$_7$R-induced pore formation, assessed by YO-PRO-1 dye uptake, was greater in BMDC, and these cells were protected from cell death. These data demonstrate that DC and macrophages display distinct patterns of cytokine regulation, particularly with respect to IL-1, as a consequence of cell-type specific differences in the physicochemical properties of the P2X$_7$R. Understanding the cell-specific regulation of these cytokines is essential for manipulating such responses in health and disease.

1. Introduction

The interleukin (IL)-1 cytokines are among the most potent initiators of inflammation and are involved in a wide variety of protective host responses against viral, fungal, parasitic and bacterial infections, but also contribute to damaging inflammatory processes in autoimmune inflammatory diseases including rheumatoid arthritis and type-2 diabetes [1,2]. The IL-1 family consists of pro- and anti-inflammatory molecules including the 3 main ligands IL-1β, IL-1α and IL-18, the natural inhibitor of IL-1α and β IL-1 receptor antagonist, the membrane-associated and decoy receptors (IL-1RI and IL-1RII, respectively) and various accessory proteins [3,4]. IL-1α and IL-1β are the main pro-inflammatory forms, and are known to initiate the synthesis of cyclooxygenase type 2, type-2 phospholipase A and inducible nitric oxide synthase, contributing to the induction of fever, vasodilation and hypotension [5]. Although most cellular responses are shared between IL-1α and β isoforms, both of which signal through the same receptor, importantly IL-1α is primarily cell associated, whereas IL-1β is secreted [6]. There are also reports of isoform-specific functions, including for example, the selective recruitment of neutrophils and macrophages being initiated by IL-1α and IL-1β, respectively [7].

The production of IL-1β is regulated at several checkpoints, including transcription, translation, maturation and secretion, in

Abbreviations: ATP, adenosine triphosphate; BM, bone marrow; BMM, bone marrow-derived macrophages; DAMPs, danger associated molecular patterns; DC, dendritic cells; DMSO, dimethyl sulfoxide; EDTA, ethylene diamine tetracetic acid; ELISA, enzyme-linked immunosorbant assay; FCS, fetal calf serum; FITC, fluorescein isothiocyanate; GM-CSF, granulocyte/macrophage-colony stimulating factor; HRPT, hypoxanthine-guanine phosphoribosyl transferase; IL, interleukin; LPS, lipopolysaccharide; MFI, mean fluorescence intensity; MHC, major histocompatibility complex; PAMPs, pathogen associated molecular patterns; PBS, phosphate buffered saline; PE, phycoerythrin; PI, propidium iodide; PM, peritoneal macrophage; PRR, pattern recognition receptors; qPCR, quantitative polymerase chain reaction; TLR, Toll-like receptor.

* Corresponding author. Tel.: +44 161 2751685; fax: +44 (0) 161 2755586.
E-mail address: rebecca.dearman@manchester.ac.uk (R.J. Dearman).

http://dx.doi.org/10.1016/j.cyto.2015.05.013
1043-4666/

order to contain and control inflammatory responses [8]. IL-1α and β expression is regulated by pattern recognition receptors (PRR) which are expressed by the immune sentinel cells that are the primary source of this cytokine (monocytes, macrophages and dendritic cells [DC]) that are specialized to recognize bacterial or viral components. A major class of PRR and one that is often manipulated experimentally are members of the Toll-like receptor (TLR) family. Upon ligation of these receptors, inactive precursor IL-1 molecules accumulate beneath the inner leaflet of the cell membrane (reviewed in [9]). IL-1α and β precursors (pro-forms) remain cytosolic until the 'primed' cell encounters an additional stimulus. In order for processing and secretion of active IL-1 cytosolic PRR are activated. These typically belong to a family of nucleotide-binding domain leucine-rich repeat containing receptors, consisting of 23 members that are activated by pathogen or damage associated molecular patterns (PAMPs or DAMPs respectively), and form multi-molecular complexes known as inflammasomes [10]. Inflammasomes facilitate activation of the protease caspase-1 that cleaves pro-IL-1β into an active form which is required for the efficient and rapid release of the cytokine into the extracellular space [11,12]. Although not a substrate for caspase-1, activation of the inflammasome also induces the processing and release of IL-1α [13].

Extracellular adenosine triphosphate (ATP) represents a physiological DAMP that induces rapid inflammasome and caspase-1 activation [14]. ATP is produced ubiquitously, is present in the cytoplasm of every cell, is hydrophilic, and its extracellular concentration is tightly regulated by ecto-ATPases, making it an ideal danger signal for potentiating immune responses [15]. The traditional view, derived mainly from studies of macrophage populations, is that ATP binds to $P2X_7R$, triggering K^+ efflux and activating inflammasome-mediated IL-1β responses [16–18]. Recently, however, it has been shown that DC may also be potential sources of $P2X_7R$ induced IL-1β and thus also contribute to IL-1-dependent inflammatory responses [19]. Thus, the main objective of the present investigation was to examine the role of the ATP-$P2X_7R$ axis in mediating inflammasome activation and IL-1 release by DC and to compare these responses with macrophages matured from the same initial precursor cell preparations.

Activation of the $P2X_7R$ is associated with a wide variety of functions beyond that of inflammasome activation and IL-1β release [20], raising the question of whether a single receptor can regulate such multiple actions. Recently, differential expression of splice variants has been shown to significantly alter the properties of the $P2X_7R$ functional trimer and has therefore been proposed as an endogenous regulatory mechanism [21,22]. The currently available anti-murine $P2X_7R$ antibodies do not discriminate between various splice variants. We have therefore examined the expression of the first reported variant ($P2X_7A$) and a gain-of-function isoform ($P2X_7K$) at the transcriptional level in murine bone marrow (BM) derived DC and BM macrophages (BMM). Additionally, on the basis that localization and stabilization of the $P2X_7R$ on the cell surface membrane, at least in microglia and macrophages, is tightly regulated by a specific sequence within a lipopolysaccharide (LPS)-binding motif [23], the effect of LPS priming on the expression of various splice variant isoforms of the receptor was investigated.

2. Materials and methods

2.1. Experimental animals

Young (6–8 weeks old) female BALB/c strain mice (obtained from Harlan Olac, Bicester, UK) were used. Mice were provided with environmental stimuli (bedding and nesting material); food (Beekay Rat and Mouse Diet No1 pellets; B&K Universal, Hull, UK) and water were available *ad libitum* and environmental conditions comprised a 12 h dark/light cycle at 21 °C ± 1 °C and 55% ± 10% humidity. Maintenance and treatment of animals were conducted as specified by the U.K. Animals (Scientific Procedures) Act 1986. Mice were sacrificed by exposure to a rising concentration of $C0_2$ gas followed by dislocation of the neck in concordance with schedule 1 (Animals [Scientific Procedures] Act 1986).

2.2. Generation and culture of BMDC and BMM from BM progenitors

BM progenitor cells were isolated and cultured as described previously [24]. BMDC (2×10^6 per 10 ml) were cultured in RPMI-1640 medium containing 25 mM HEPES, 400 μg/ml penicillin/streptomycin, 292 μg/ml L-glutamine, 0.1% (v/v) 2-mercaptoethanol and 10% (v/v) heat inactivated fetal calf serum (FCS) (RPMI-10% FCS; all supplied by Invitrogen, California, USA) containing 20 ng/ml granulocyte/macrophage-colony stimulating factor (GM-CSF) (Peprotech, New Jersey, USA). BMM were cultured under the same conditions, except DMEM medium (Sigma–Aldrich, Poole, Dorset, UK) was supplemented with 30% L-929 conditioned medium in place of GM-CSF. Medium was refreshed every 3 days, and cells were harvested on day 8 by gentle agitation (BMDC) or following treatment with ethylene diamine tetraacetic acid (EDTA) (0.25%, Sigma–Aldrich) (BMM). Viable cell counts were performed by trypan blue exclusion and cells were seeded into 24-well tissue culture plates at 1×10^6 cells per well.

Cells prepared as described above were cultured in the presence of various reagents: LPS (*Escherichia coli* serotype 055:B5; Sigma–Aldrich), ATP (stored at −20 °C as stock solution prepared at 100 mM and pH adjusted to 7.5; Sigma–Aldrich), the $P2X_7R$ inhibitor A-740003 (Tocris Bioscience, Bristol, UK; dissolved in 0.5% dimethyl sulfoxide [DMSO]), or apyrase (Sigma–Aldrich). Cells were cultured with 1 or 1000 ng/ml LPS for 2 h, for the last 30 min of the incubation in the presence of 0–10 mM ATP or 2–20 μg/ml of apyrase. Cells that were treated with the $P2X_7R$ inhibitor A-740003 received various concentrations (0.1–100 μM) in DMSO or DMSO alone for 10 min prior to the addition of ATP. At the end of every series of treatments, supernatants were collected and the remaining cell pellets were lyzed with 100 μl/well of lysis buffer (20 mM Tris–HCl, 137 mM NaCl, 20 mM EDTA, 10% glycerol, 0.5% Ipegal, phenylmethylsulfonyl [1 mM] and protease inhibitor cocktail [1:100] (Calbiochem, San Diego, USA)) and lysates collected.

2.3. Cell viability assessment

The viability of cell populations after treatment with LPS or ATP was assessed by propidium iodide (PI, 10 μg/ml; Sigma–Aldrich) exclusion and analysis by flow cytometry or by trypan blue exclusion and analysis by light microscopy. In some experiments, viability was assessed using lactate dehydrogenase (LDH) activity in cultured, cell-free supernatants using the cytotoxicity detection kit (ROCHE; Basel, Switzerland) according to the manufacturer's instructions. The LDH enzyme is stably expressed in most cells and it is rapidly released when the plasma membrane is perturbed. Therefore, an increase in LDH activity in cultured supernatants correlates to an increase in the number of dying/dead cells in culture. Cell viability was determined using an equation that compared the LDH levels detected in the sample of interest to those obtained from a "positive control" (cell-free supernatants collected from freeze–thawed cells of the same type, BMDC or BMM and of equal number) and a "negative control" (cell-free culture medium).

Please cite this article in press as: Englezou PC et al. $P2X_7R$ activation drives distinct IL-1 responses in dendritic cells compared to macrophages. Cytokine (2015), http://dx.doi.org/10.1016/j.cyto.2015.05.013

$$\% \text{ cytotoxicity} = \frac{(\text{LDH activity in sample of interest} - \text{LDH activity in negative control})}{(\text{LDH activity in positive control} - \text{LDH activity in negative control})}$$

2.4. Flow cytometric analyses for phenotypic markers

Cells (2×10^5) were stained with antibodies directed against major histocompatibility complex (MHC) class II (clone 2G9, rat IgG_{2a}; 2.5 μg/ml), phycoerythrin (PE)-labelled hamster anti-mouse CD11c (IgG1κ; 4 μg/ml), PE-labelled anti-mouse CD11b (rat IgG_{2a}; 10 μg/ml), or isotype controls (rat IgG_{2a}, rat IgG_{2b} or PE-labelled hamster IgG1κ; all from BD Biosciences, Princeton, New Jersey, USA), or with PE-labelled anti-mouse F4/80 (rat IgG_{2a}; 4 μg/ml; E Biosciences, Hatfield, UK). For unlabelled primary antibodies, cells were stained subsequently with goat anti-rat IgG fluorescein isothiocyanate (FITC)-labelled polyclonal antibody (7 μg/ml; AbD Serotec, Kidlington, Oxford, UK). Incubations and washes were performed in 5% FCS in phosphate buffered saline (PBS) at 4 °C. Cells were re-suspended in sodium azide buffer (0.05% sodium azide and 1% FCS). A FACScalibur machine and *CellQuest Pro* software (BD Biosciences) were used to analyze 10^4 cells and PI was used to exclude dead cells from analysis and matching isotype control staining was used to set gates. Data were expressed as % positive cells and as mean fluorescence intensity (MFI).

2.5. Western blot analysis of $P2X_7R$ and IL-1β expression

Cell lysates were prepared from cultured BMDC (1×10^6), BMM or HEK-293 cells, and from freshly isolated peritoneal macrophages (PM) (adherent peritoneal exudate population) or splenocytes (prepared by mechanical disaggregation and ammonium chloride lysis). Supernatants and lysates were diluted in sample buffer (BioRad) containing 1% 2-mercaptoethanol and heated at 80 °C for 5 min. Protein concentration was determined by modified Lowry (Bio-Rad, Berkeley, California, USA), and samples (20 μg protein) were resolved on a 10% sodium dodecyl sulfate polyacrylamide gel. The primary antibodies were rabbit anti-mouse $P2X_7R$ (Alomone, Jerusalem, Israel; 3 μg/ml), or goat anti-mouse IL-1β antibody (R&D Systems; Abingdon, UK; 0.1 μg/m) and the secondary antibodies were horse radish peroxidase-conjugated goat anti-rabbit IgG (AbD Serotec) or horse radish peroxidase-conjugated rabbit anti-goat IgG antibody (DAKO, Copenhagen, Denmark): 50 ng/ml or 0.25 μg/ml, respectively. A Super Signal West Pico chemiluminescent substrate (Thermo Fisher Scientific, Waltham, Massachusetts, USA) was used to visualize protein expression using hyperfilm (Amersham Biosciences/GE Healthcare, Little Chalfont, Buckinghamshire, UK) and a medical film processor (Xograph Imaging System, Compact).

2.6. Electrophysiological recordings

BMDC were stained with PE-labelled anti-CD11c antibody and individual positive cells were voltage-clamped to measure ion currents following $P2X_7R$ activation. Recording pipettes were prepared from borosilicate glass (Harvard Apparatus, Kent, UK) with resistances of 2–5 MΩ. The intracellular pipette solution contained: 147 mM NaCl, 10 mM HEPES and 10 mM EGTA. The extracellular recording solution contained 147 mM NaCl, 10 mM HEPES, 13 mM glucose, 2 mM KCl, 2 mM $CaCl_2$ and 1 mM $MgCl_2$. All solutions were maintained at 300–320 mOsm/L and pH 7.3 (adjusted with NaOH). Whole-cell patch clamp recordings were made at room temperature using a HEKA EPC9 patch clamp amplifier and *Pulse* acquisition software (HEKA Elektronik GmbH, Lambrecht, Germany) at a holding potential of −60 mV. The data were low-pass filtered at 3 kHz and sampled at 1 kHz. ATP and A-740003 were applied using an RSC-160 rapid perfusion system (BioLogic, Claix, France), with orifices positioned approximately 100 nm away from the cell under investigation.

2.7. YO-PRO-1 dye uptake assay

Concurrent cultures of day 8 BMDC or BMM were transferred into 96-well tissue culture plates (black with clear bottom) at 3×10^5 cells per 0.2 ml and incubated overnight at 37 °C and 5% CO_2 and allowed to adhere. Cells were either untreated or primed with 1000 ng/ml of LPS for 2 h and washed with PBS before the addition of 100 μl/well of YO-PRO-1 (10 μM; Tocris Bioscience) solution, prepared in standard extracellular solution (136 mM NaCl, 1.2 mM KH_2PO_4, 1.2 mM $MgSO_4$, 1.8 mM KCl, 1.2 mM $CaCl_2$, 5 mM $NaHCO_3$, 20 mM HEPES and 5.5 mM of glucose). Fluorescence (495 nm/515 nm excitation/emission) was monitored using a fluorescent laser imaging plate reader (Flex Station 3; Molecular Devices, San Francisco, USA). After recording a baseline current flow for a 30 s interval, ATP at 1 or 5 mM was applied to LPS primed or unprimed cells. YO-PRO-1 fluorescence was measured at 3 s intervals throughout the procedure and a mean fluorescence value was obtained for triplicate wells.

2.8. Cytokine enzyme-linked immunosorbant assay (ELISA)

Lysate (intracellular) and supernatant (secreted) IL-1α and IL-1β levels were determined using DuoSet ELISA kits (R&D systems) according to the manufacturer's instructions. The DuoSet antibodies did not differentiate between precursor and mature forms of IL-1. IL-6 content was measured using a specific mouse sandwich ELISA (as described in [25]). The lower limits of accurate detection for IL-1 and IL-6 were approximately 40 and 80 pg/ml, respectively.

2.9. Analysis of $P2X_7R$ splice isoform expression by quantitative-polymerase chain reaction (q-PCR)

Total RNA was extracted from the cell populations of interest using an RNA isolation system (TRIzol RNA minikit, Invitrogen) according to the manufacturer's instructions and subsequently treated with DNase (Ambion, Life Technologies, Carlsbad, California, USA). An equal amount of RNA (300 ng) was reverse transcribed using a high capacity RNA-to-cDNA kit (Invitrogen). A dye based (SYBR Green) qPCR was used to obtain relative quantification of mRNA levels of the various $P2X_7R$ isoforms of interest relative to the housekeeping gene hypoxanthine–guanine phosphoribosyltransferase (HRPT). (HPRT: forward: GGG CTT ACC TCA CTG CTT TC, reverse: TCT CCA CCA ATA ACT TTT ATG TCC; $P2X_7A$: forward: CAC ATG ATC GTC TTT TCC TAC, reverse: GGT CAG AAG AGC ACT GTG C; $P2X_7K$: forward: GCC CGT GAG CCA CTT ATG C reverse: GGT CAG AAG AGC ACT GTG C. All primers were obtained from Sigma–Aldrich and were checked against GenBank for selectivity. A melt curve was also performed for all primers to ensure that they recognized and amplified a single product. qPCR reactions were performed using a SensiFAST no-ROX Kit (Life Technologies) according to the manufacturer's instructions. All samples were run in triplicate in an ABI StepOnePlus PCR machine (Applied Biosystems, Life Technologies) using the following

Please cite this article in press as: Englezou PC et al. $P2X_7R$ activation drives distinct IL-1 responses in dendritic cells compared to macrophages. Cytokine (2015), http://dx.doi.org/10.1016/j.cyto.2015.05.013

conditions: 95 °C for 2 min and then 40 cycles at: 95 °C for 5 s (denaturation), 60–65 °C for 10 s (annealing) and 72 °C for 5–20 s (elongation). Samples were considered positive if the amplification curve crossed the set threshold (set automatically). Fold changes in gene expression for each $P2X_7R$ splice isoform were normalized to the housekeeping gene (HPRT) and calculated using the $2^{-\Delta\Delta CT}$ method. PCR samples along with a 100 bp interval ladder (BIOLINE, London, UK) were separated on a 1% agarose gel with ethidium bromide dissolved in TBE buffer (Promega). The bands were visualized using a UV-transluminator (Syngene, Cambridge, UK) and photographed using a polaroid camera.

2.10. Data analyses

Data were analyzed using Prism 6.0 and multiple comparisons were considered using one-way ANOVA. A two-tailed Student's *t*-test was employed for comparisons between two different groups. Dunnett's multiple comparison post-hoc test was employed for comparisons with a control group. Tukey's test was employed when comparisons were made between all treatment groups and two-way ANOVA and Sidak's multiple comparison post-hoc tests were employed for comparisons between different treatments of two cell types of interest. Significant differences are illustrated by $*p < 0.05$.

3. Results

3.1. Phenotypic differences between BMDC and BMM

Membrane marker protein expression of day 8 BMDC and BMM isolated in parallel from the same progenitor cells was characterized by flow cytometry (Fig. 1). Consistent with previous reports [24] the majority of BMDC displayed a DC phenotype expressing relatively high levels of MHC class II and the DC associated marker CD11c, but low levels of the macrophage marker F4/80 (Fig. 1b and c). In contrast, BMM exhibited a typical macrophage profile with high levels of F4/80 and low levels of both MHC class II and CD11c (Fig. 1b and c). Both cell types (~90%) displayed similar levels of CD11b, an integrin found on macrophages and some DC populations (Fig. 1). These BMDC and BMM cell populations were analyzed for $P2X_7R$ expression at the level of transcription (by qPCR, data not shown) and protein (by Western blotting), the latter using a polyclonal rabbit antibody with specificity for a $P2X_7R$ intracellular terminus epitope (Fig. 2a). Cell lysates were

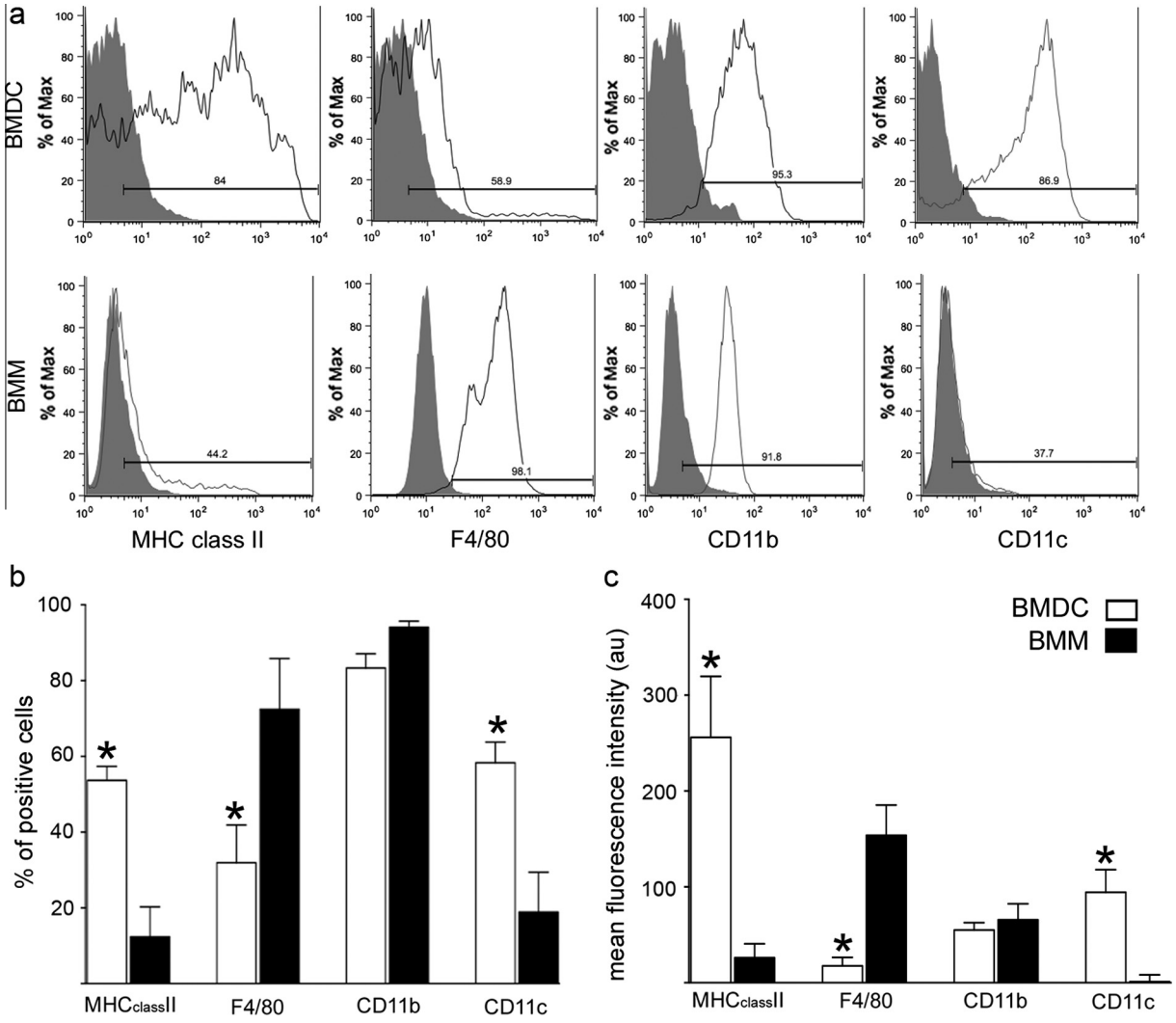

Fig. 1. Phenotypic characterization of murine BMDC and BMM. BMDC (□) and BMM (■) were harvested after 8 days of culture and 10^4 cells analyzed by flow cytometry for surface of expression of MHC class II, CD86 (data not shown), F4/80, CD11b and CD11c. Data are shown as (a) representative histograms, where closed histograms represent the isotype controls, and with respect to (b) the percentage of positive cells and (c) MFI (arbitrary units) and are displayed as mean ± SEM ($n = 3$ independent experiments). The statistical significance of differences between BMDC and BMM was assessed by one-way ANOVA and Dunnett's multiple comparison post hoc test ($* = p < 0.05$).

Please cite this article in press as: Englezou PC et al. $P2X_7R$ activation drives distinct IL-1 responses in dendritic cells compared to macrophages. Cytokine (2015), http://dx.doi.org/10.1016/j.cyto.2015.05.013

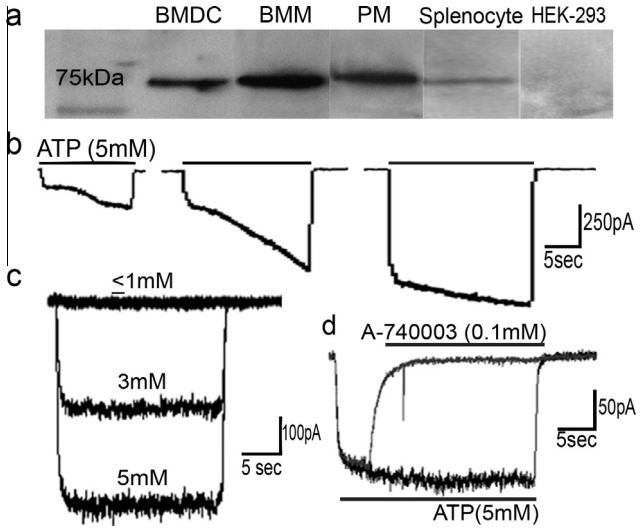

Fig. 2. CD11c$^+$ murine BMDC display functional P2X$_7$R. Cell lysates were collected from 10^6 day 8 BMDC or BMM or HEK-293 cells (negative control), or from an equivalent number of freshly isolated splenocytes or PM. Parallel aliquots of cells were lyzed and equivalent amounts of protein (20 μg) from each cell type were analyzed for P2X$_7$R expression by Western blotting. Representative images from the same analysis are shown. A total of three independent preparations were analyzed (data not shown). Images were cropped and reordered (a). mRNA expression of P2X$_7$R was also evaluated for each cell population using qPCR. The same pattern was detected at the level of message (data not shown). Day 8 BMDC at 0.25×10^6/ml were cultured on glass coverslips and stained with anti-CD11c antibody to identify CD11c$^+$ cells before individual cells were patch clamped. Representative traces showing current facilitation in clamped CD11c$^+$ BMDC following repeated applications of ATP at 5 mM (for 30 s at 30 s intervals) are shown (b). ATP was applied at ⩽1 mM, 3 mM and 5 mM to fully facilitated CD11c$^+$ BMDC channels (representative traces from $n = 6$ experiments) (c). Responses to 5 mM ATP were measured in the presence and absence of the specific P2X$_7$R inhibitor, A-740003 (0.1 mM). A-740003 was applied for 20 s during a sustained application of ATP (5 mM, 30 s), as shown. An ATP control recording (30 s) was made 30 s before the addition of A-740003 (representative traces from $n = 6$ experiments are shown) (d).

prepared from day 8 BMDC and BMM, from freshly isolated PM and unfractionated splenocytes. Negative control lysates were obtained from cultured HEK-293 cells that do not express P2X$_7$R. qPCR and Western blotting, respectively, revealed the presence of P2X$_7$A mRNA (data not shown) and protein at the appropriate molecular weight (75 kDa) in all cell types apart from the HEK-293 lysates (Fig. 2a).

3.2. Murine CD11c$^+$ BMDC express a functional P2X$_7$R receptor

Although P2X$_7$R expression in BMDC lysates was shown using Western blotting, given that ~30% of the BMDC population did not express CD11c, it was necessary to demonstrate at the single cell level CD11c positivity and P2X$_7$R functionality, measured electrophysiologically by patch clamping. Day 8 BMDC were stained for CD11c expression and individual CD11c$^+$ cells were voltage-clamped *in situ*. Current facilitation (increase in current amplitude in response to consecutive agonist applications) is a characteristic property of the P2X$_7$R [26] and is consistent with the findings that the amplitude of inward BMDC current increased 2-fold during each of three consecutive applications of ATP (Fig. 2b; representative traces for 5 mM ATP at 30 s intervals). Whole-cell currents recorded during application of ATP (0.1–5 mM, 20 s) revealed dose dependent responses (Fig. 2c; representative traces). Inward currents of 3.2 ± 0.7 and 6.1 ± 1.0 pA/pF ($n = 7$) were observed in response to 3 and 5 mM ATP, respectively, whereas ⩽1 mM ATP failed to elicit a detectable current. The effect of the specific P2X$_7$R inhibitor, A-740003, on ATP-evoked currents in BMDC was also investigated (Fig. 2d; representative traces). A-740003 (0.1 mM, 20 s) was co-applied with ATP (5 mM, 30 s), and significantly inhibited currents evoked by ATP alone by 93 ± 2% ($n = 6$; $p < 0.05$).

3.3. Different P2X$_7$R-induced IL-1 cytokine responses in BMDC and BMM

Subsequently the ability of LPS and ATP to induce IL-1 expression and release by BMDC and BMM was examined. Cells were primed with low (1 ng/ml) or high (1000 ng/ml) dose LPS for 90 min followed by a 30 min incubation with ATP (0.5–10 mM). IL-1β levels were quantified in both lysates (i.e. intracellular content) (Fig. 3a and b) and supernatants (reflecting cytokine release) (Fig. 3c and d). There was no detectable cytokine expression following culture with medium or ATP alone at any concentration with either cell type (data not shown). BMM were more sensitive to LPS priming than were BMDC, at least with respect to intracellular cytokine production. At the lower LPS dose (1 ng/ml), there was little IL-1β detected in either lysates or supernatant following treatment of BMDC whereas BMM were primed successfully with approximately 4 ng/ml of cytokine detected in the lysate. However, challenge with ATP did not provoke detectable secretion, instead concentrations of 5 mM ATP and above resulted in decreased intracellular cytokine content. For both cell types there was significant priming with high dose LPS, with approximately 20 ng/ml IL-1β recorded in lysates following incubation with LPS alone. Here BMDC were more responsive than BMM with respect to both maximal amounts of secreted product (16 ng/ml versus 2 ng/ml) and the minimum amount of ATP that induced significant secretion (1 versus 5 mM). Furthermore, BMDC tolerated the high dose of ATP, with maximal secretion still recorded after challenge with 10 mM ATP, whereas BMM were unable to secrete IL-1β under the same conditions. For both cell types, ATP-induced cytokine secretion was associated with a concomitant drop in intracellular IL-1β levels. In order to exclude the possibility that IL-1β release was simply due to ATP-induced cytotoxicity, following detachment of both cell populations with EDTA, viability was assessed by PI staining (Fig. 3e and f). ATP treatment did not significantly affect BMM viability, whereas for BMDC there was a marked reduction (from 95% to 50%) in viability only when cells were primed with 1000 ng/ml LPS and challenged with 5 mM ATP. Interestingly, incubation with 10 mM ATP did not affect cell viability.

Given the marked reduction in viability (assessed by PI exclusion) recorded for BMDC challenged with 5 mM ATP, alternative measures of viability were explored. Release of LDH was an appropriate endpoint for the measurement of BMM viability, with LDH assay results paralleling those obtained with PI exclusion (no marked effect of ATP)(data no shown). However, this endpoint was not of utility for the measurement of BMDC viability. Although there was apparently little impact of treatment with either LPS or ATP on the viability of BMDC compared with medium-treated controls with respect to LDH release, the baseline viability of untreated BMDC was apparently very low (~20% viable). Therefore BMDC viability was assessed using trypan blue exclusion (Fig. 4a). These data demonstrated that although there was a small drop in viability following LPS treatment, the addition of ATP in the concentration range utilized herein (0.5–10 mM) was without significant effect on cell viability. The same pattern of IL-1β expression was recorded as that observed previously: LPS-stimulated BMDC expressed intracellular cytokine and ATP challenge was necessary for the secretion of IL-1β (Fig. 4b). Furthermore, Western blot analysis of lysates and supernatants confirmed that intracellular IL-1β detected in LPS primed cells was all in the precursor, pro-IL-1β form (Fig. 4c; representative blot). Non-specific binding was also evident in the analysis of

Please cite this article in press as: Englezou PC et al. P2X$_7$R activation drives distinct IL-1 responses in dendritic cells compared to macrophages. Cytokine (2015), http://dx.doi.org/10.1016/j.cyto.2015.05.013

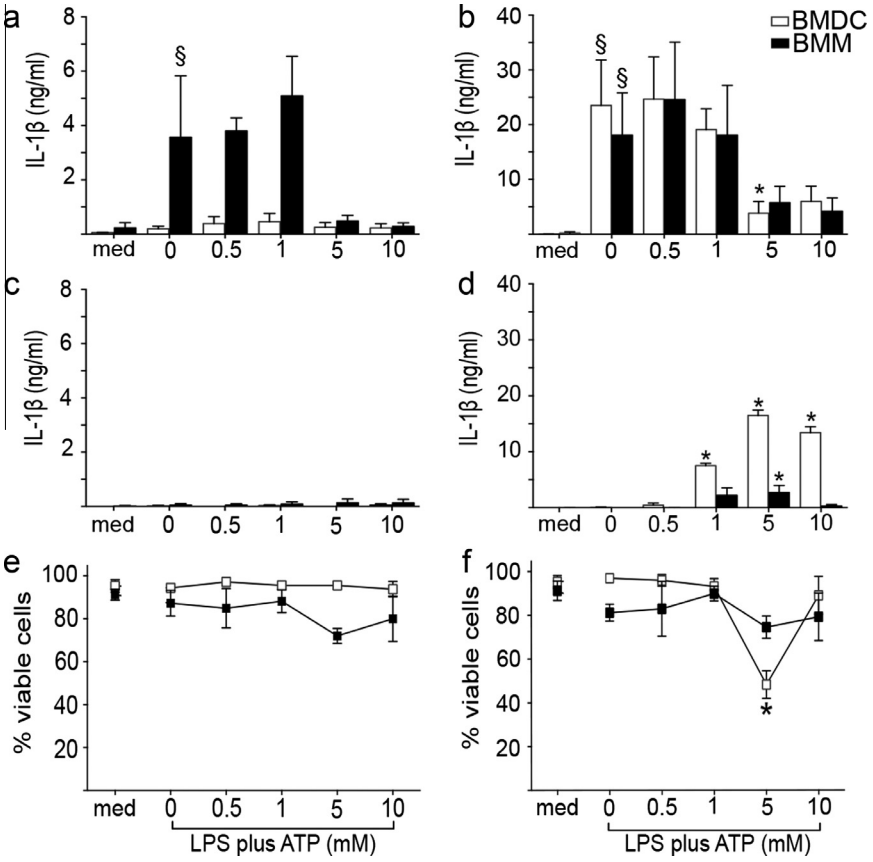

Fig. 3. Differential IL-1β production and secretion by BMDC and BMM following LPS priming and ATP activation. Day 8 BMDC (□) and BMM (■) at 10^6/ml were cultured for 2 h with 1 (a, c, e) or 1000 ng/ml (b, d, f) LPS then challenged for the last 30 min with ATP at 0, 0.5, 1, 5 or 10 mM. Negative control cells were cultured with medium alone throughout (med). Intracellular (a, b) and secreted (c, d) levels of IL-1β were quantified by cytokine-specific ELISA. Cells were stained with PI and cell viability of BMDC (□) and BMM (■) was assessed by flow cytometry (e, f). Data shown are mean ± SEM ($n = 3$ independent experiments). Statistical significance of differences within BMDC/BMM populations between medium- and LPS alone-treated cells was considered by a two-tailed Student's t-test (§ = $p < 0.05$) and between the LPS-treated groups (LPS alone-treated cells were used as the comparator) was assessed by one way ANOVA and Dunnett's multiple comparison post-hoc test (∗ = $p < 0.05$).

BMDC supernatants due to the presence of FCS, since the same non-specific band without bands at the right size for mature or pro-IL-1beta was also detected when medium/FCS alone was analyzed (data not shown). Upon stimulation of LPS-primed cells with 5 mM or 10 mM ATP, IL-1β was detected in both lysates and supernatants. The cytokine in the lysates was the precursor (31 kDa) form whereas in the supernatants it was primarily in the mature, 17 kDa processed form.

IL-1α production and release was also monitored for the same experimental protocol (Fig. 5a and c). The pattern of IL-1β and IL-1α production was similar as were the dose response profiles. Thus, high dose LPS primed BMDC for IL-1α production (intracellular expression) but significant secretion was only observed following challenge with ATP, and this was paralleled by a reduction in cytokine content of lysates. BMM were considerably less effective at producing this cytokine (2 versus 9 ng/ml in lysates and <0.2 versus 6 ng/ml in supernatants). Expression of IL-6, a pro-inflammatory cytokine that does not share the same inflammasome-associated pathway of secretion as the IL-1 family, was also investigated (Fig. 5b and d). Only LPS-primed BMDC were able to elaborate IL-6, which was secreted without any requirement for ATP challenge.

The $P2X_7R$ specific inhibitor A-740003 was employed to validate the role of $P2X_7R$ signalling in LPS/ATP-induced IL-1 production by BMDC and BMM under conditions optimal for IL-1 release (priming with 1000 ng/ml LPS and challenge with 5 mM ATP; Fig. 6). As described above (cf. Figs. 3 and 5), LPS priming of BMDC resulted in significant up-regulation of both isoforms of IL-1, but was unable to cause secretion. Treatment with ATP resulted in secretion (~15 ng/ml) and a concomitant drop in intracellular cytokine levels, which was blocked almost completely (>95% inhibition) by the addition of 0.1 mM A-740003. The inhibitory effects on IL-1β production by BMM were similar, with effective blocking with A-740003 (91%), although ATP-induced secretion was less robust (~1 ng/ml), and BMM were ineffective at upregulating IL-1α production. With regards to IL-6 expression (data not shown), activation with exogenous ATP (5 mM) had no significant effect on IL-6 release and, importantly, neither did treatment with A-740003. Also consistent with previous experiments, treatment of BMM with ATP was without significant toxicity (viability varied between 90% and 80% regardless of treatment), whereas BMDC displayed a reduction in cell viability as measured by PI exclusion upon ATP treatment (from 95% to 60%) which was reversed by incubation with the $P2X_7R$ inhibitor.

In order to exclude a role for adenosine diphosphate or monophosphate signalling in mediating IL-1 secretion from LPS-primed BMDC, the ATP-degrading enzyme, apyrase, was employed [27]. LPS-primed BMDC were treated with apyrase immediately prior (30 s) to challenge with 1 mM ATP and IL-1α and β production assessed (Fig. 6e and f). Apyrase was without significant effect on cell viability (data not shown) or intracellular cytokine content, but caused a dose dependent inhibition of secretion of both cytokines, with significant inhibition (>90%) recorded at 20 μg/ml. However, apyrase did not impact on the more

Please cite this article in press as: Englezou PC et al. $P2X_7R$ activation drives distinct IL-1 responses in dendritic cells compared to macrophages. Cytokine (2015), http://dx.doi.org/10.1016/j.cyto.2015.05.013

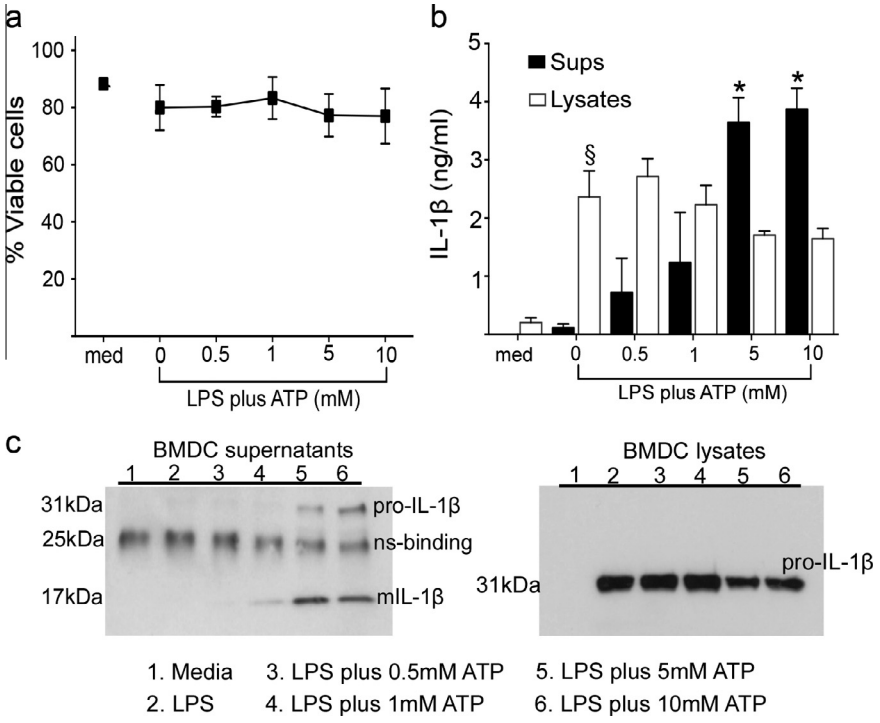

Fig. 4. BMDC secrete mature IL-1β following LPS priming and ATP. Day 8 BMDC at 10^6/ml were cultured for 2 h with 1000 ng/ml LPS then challenged for the last 30 min with ATP at 0, 0.5, 1, 5 or 10 mM. Negative control cells were cultured with medium alone throughout (med). Viability was assessed by trypan exclusion (a) and intracellular and secreted levels of IL-1β were quantified by cytokine-specific ELISA (b). Data shown are mean ± SEM (n = 2 for 0.5 and 1 mM ATP with regards to cytokine analysis and n = 3 for all other groups, independent experiments). Statistical significance between medium- and LPS alone-treated cells was considered by a two-tailed Student's t-test (§ = $p < 0.05$) and between the LPS-treated groups (LPS alone-treated cells were used as the comparator) was assessed by one way ANOVA and Dunnett's multiple comparison post-hoc test (∗ = $p < 0.05$). Parallel aliquots of cells were lyzed and equivalent amounts of lysate protein (20 μg) and supernatants were analyzed for IL-1β expression by Western blotting. Representative images from the same analysis are shown. A total of three independent preparations were analyzed (data not shown). Images were cropped (c). The band at ~25 kDa that is present in all supernatant samples represents non-specific binding to elements in the FCS. A protein marker lane on each gel was used to determine molecular weights of bands.

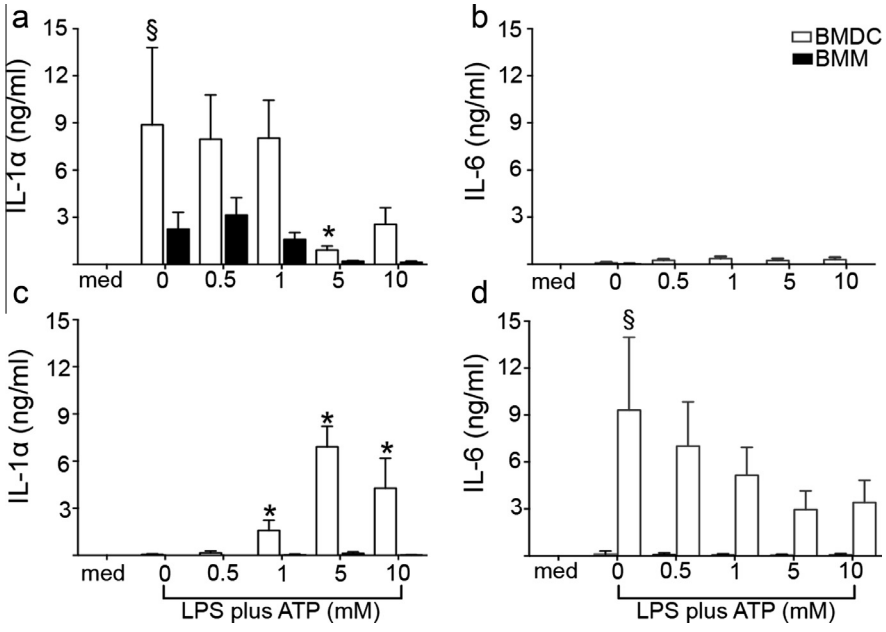

Fig. 5. BMDC and BMM IL-1α and IL-6 responses following LPS priming and ATP challenge. Day 8 BMDC (□) and BMM (■) at 10^6/ml were cultured for 2 h in the presence of medium alone (med) or LPS (1000 ng/ml) and challenged for the last 30 min with ATP at 0, 0.5, 1, 5 and 10 mM. Both intracellular (a, b) and secreted (c, d) levels of IL-1α (a, c) and IL-6 (b, d) were quantified by cytokine-specific ELISA. Data shown are mean ± SEM (n = 3 independent experiments). Statistical significance of differences within BMDC/BMM populations between medium- and LPS alone-treated cells was considered by a two-tailed Student's t-test (§ = $p < 0.05$) and between the LPS-treated groups (LPS alone-treated cells were used as the comparator) was assessed by one way ANOVA and Dunnett's multiple comparison post-hoc test (∗ = $p < 0.05$).

Please cite this article in press as: Englezou PC et al. P2X$_7$R activation drives distinct IL-1 responses in dendritic cells compared to macrophages. Cytokine (2015), http://dx.doi.org/10.1016/j.cyto.2015.05.013

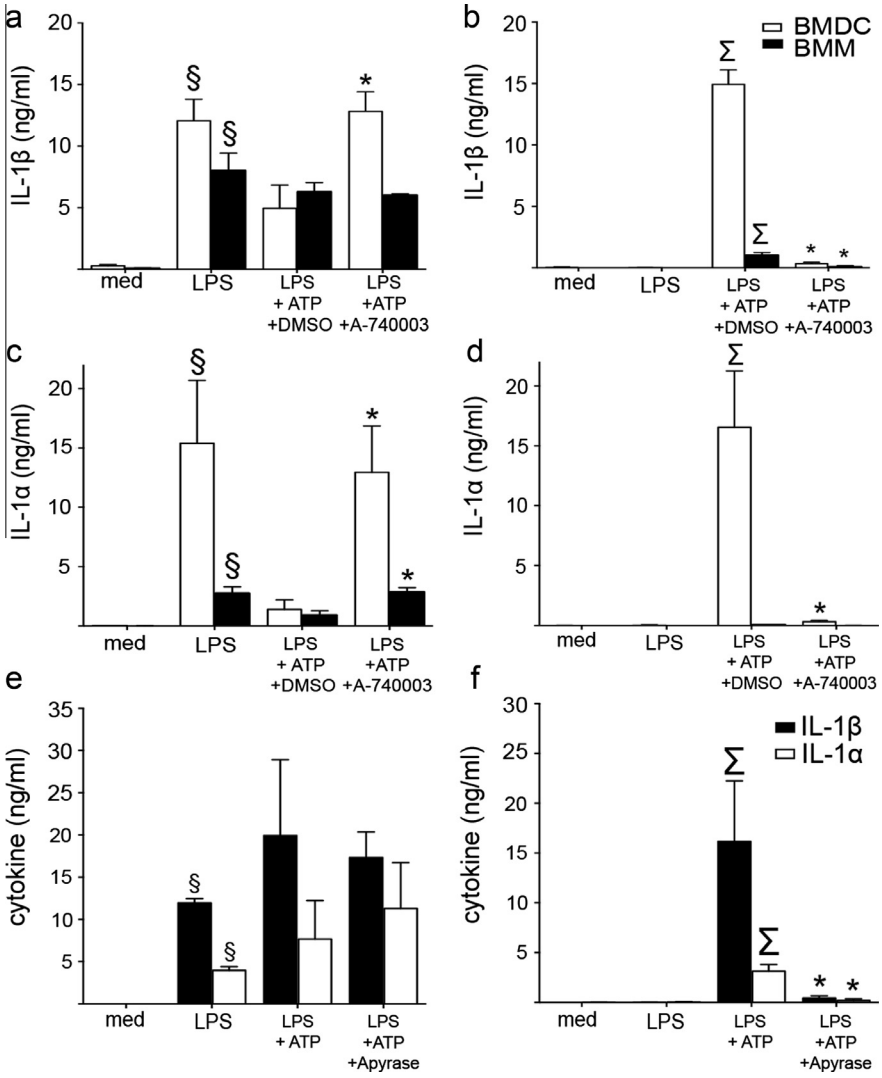

Fig. 6. Impact of $P2X_7R$ inhibition or apyrase treatment on IL-1β expression by BMDC and BMM. BMDC and BMM at 10^6/ml were cultured for 2 h in the presence of LPS (1000 ng/ml). Approximately 30 min before the end of culture, cells were treated with DMSO (0.5%) or with A-740003 (0.1 mM) formulated in DMSO (a–d). For the final 20 min of culture, selected wells were challenged with 5 mM of ATP or were untreated. Negative control cells were cultured in the presence of medium alone throughout (med). Alternatively, LPS-activated BMDC were treated with medium or apyrase (2, 20 μg/ml) immediately (30 s) before they were challenged with ATP at 1 mM for the final 20 min of culture (e, f). Intracellular (a, c, e) and secreted (b, d, f) levels of IL-1β (a, b, e (■), f (■)) and IL-1α (c, d, e, (□), f (□)) were quantified by cytokine-specific ELISA. Data shown are mean ± SEM (n = 3 independent experiments). Statistical significance of differences within BMDC/BMM populations (a–d) between medium- and LPS alone-treated cells (§ = $p < 0.05$), between LPS-primed and LPS-primed/ATP challenged cells (Σ = $p < 0.05$) and between LPS-primed/ATP-challenged cells treated with DMSO or with A-740003 (∗ = $p < 0.05$) were considered by paired two-tailed Student's t-test. For apyrase experiments (e, f) for each cytokine the statistical significance of differences between medium- and LPS alone-treated cells (§ = $p < 0.05$), LPS-primed and LPS-primed/ATP challenged cells (Σ = $p < 0.05$) and between LPS-primed/ATP-challenged cells treated with medium or apyrase/A-740003 (∗ = $p < 0.05$) were considered by paired two-tailed Student's t-test.

vigorous cytokine release induced by higher doses of ATP (5 mM), and it was not possible to use higher concentrations of enzyme as these were cytotoxic (data not shown).

3.4. $P2X_7R$ splice variant profiles are similar for BMDC and BMM

The role of expression of distinct $P2X_7R$ splice variants in the differential responses of BMDC and BMM was investigated using qPCR (Fig. 7a and b). Levels of transcripts of the different receptor isoforms were normalized to expression in unfractionated freshly isolated splenocytes. Both cell types displayed similar baseline levels of $P2X_7K$ mRNA to those found in splenocytes, but expressed some 100-fold and 1000-fold higher levels of $P2X_7A$, respectively. LPS activation was without impact on $P2X_7K$ transcripts, whereas expression of $P2X_7A$ was markedly down-regulated (approximately 10-fold) on both cell types and to similar extents.

3.5. Differential pore formation characteristics of the receptor in BMDC and BMM

Another characteristic property of the $P2X_7R$ is progressive pore dilation during sustained receptor activation [28]. This dilation increases the permeability of the receptor to large fluorescent dyes such as YO-PRO-1, leading to extracellular dye uptake. BMDC $P2X_7R$ dilation was compared with that of the well-characterized BMM $P2X_7R$ using a YO-PRO-1 uptake assay developed on the Flexstation-3 fluorescent plate reader (Fig. 7c and d). At first, lower concentrations (1μM) of YO-PRO-1 were investigated, but such did not achieve sufficient sensitivity for analysis. At higher concentrations (10μM) of YO-PRO-1, both BMDC (Fig. 7c) and BMM (Fig. 7d) were seen to accumulate YO-PRO-1 in response to ATP (1 mM, 90 min), measured as a function of a time-dependent increase in fluorescence; no uptake was observed in the absence of ATP. LPS

Please cite this article in press as: Englezou PC et al. $P2X_7R$ activation drives distinct IL-1 responses in dendritic cells compared to macrophages. Cytokine (2015), http://dx.doi.org/10.1016/j.cyto.2015.05.013

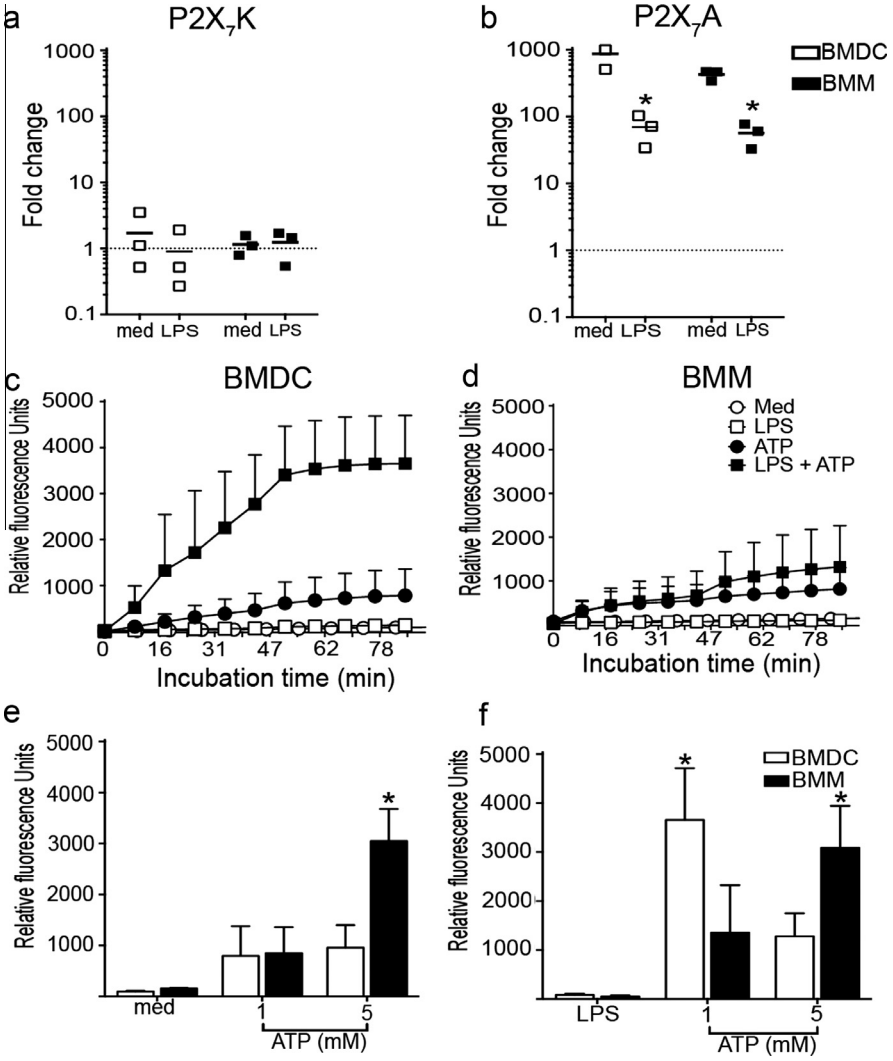

Fig. 7. $P2X_7R$-induced pore formation and splice variant expression profiles in BMDC and BMM. Cells (10^6/ml) were incubated in medium alone (med) or in the presence of LPS (1000 ng/ml) for 2 h. mRNA expression levels for each splice variant were measured using qPCR. Levels of mRNA for (a) $P2X_7K$ and (b) $P2X_7A$ were normalized to the expression levels of the housekeeping gene, HPRT, and are expressed as fold changes relative to expression levels detected in unfractionated splenocytes. Data are shown as mean (±SEM) and three independent BMDC (□) and BMM (■) preparations. Statistical significance of differences between groups within BMDC/BMM populations was assessed with a paired two-tailed Student's *t*-test (∗ = $p < 0.05$). BMDC (c) and BMM (d) at 0.3×10^6/ml were incubated in medium alone or in the presence of 1000 ng/ml LPS for 2 h and subsequently challenged with 1 mM ATP or with medium for up to 90 min (medium alone ○; LPS alone, □; medium/ATP, ●; LPS/ATP, ■). Time-dependent YO-PRO-1 dye uptake was recorded as changes in fluorescence measured at 3 s intervals for 90 min, using a Flex Station 3. Traces are presented as relative fluorescence units over time. The same experimental setup was used to measure cumulative levels of dye uptake (relative fluorescence units) for medium-treated (e) or LPS-treated (f) BMDC (open columns) and BMM (closed columns) 85 min post challenge with 1 mM or 5 mM ATP. Data shown are mean ± SEM ($n = 3$ independent experiments). Statistical significance of differences within BMDC/BMM populations was considered between the various groups (using ATP-treated cells or LPS-treated cells as a comparator) at 85 min post ATP activation and assessed by one way ANOVA and Dunnett's multiple comparison post-hoc test (∗ = $p < 0.05$).

priming BMDC increased ATP-induced YO-PRO-1 uptake considerably but was without effect on dye uptake by BMM. Additionally, LPS alone was not sufficient to elicit YO-PRO-1 uptake by either cell type. This pattern of YO-PRO-1 uptake was confirmed when the cumulative levels of dye uptake were quantified in medium-treated and LPS-primed BMDC and BMM in the presence or absence of 1 mM ATP challenge (Fig. 7e and f). Interestingly, however, challenge with 5 mM ATP abrogated the LPS priming effect for BMDC whereas BMM displayed enhanced dye uptake in the presence of 5 mM ATP regardless of LPS priming (Fig. 7f).

4. Discussion

These investigations have focused on characterizing $P2X_7R$ expression and functional activity, principally via the secretion of IL-1, by murine BMDC in comparison with BMM. $P2X_7R$ expression by both cell types was established by Western blot analysis and qPCR. More precisely, Western blot analysis revealed expression of a 75 kDa protein in BMDC and BMM suggesting the presence of full-length wild type receptor ($P2X_7A$) or gain-of-function variants such as the $P2X_7K$. Although efforts were made to detect protein expression with an antibody directed against an epitope situated in the extracellular loop of the protein thereby enable further investigations expression of different variants at the protein level, this proved unsuccessful (data not shown). The presence of $P2X_7R$ splice variants was therefore addressed at the mRNA level and is discussed below. Loss-of-function $P2X_7R$ variants have been shown to lack most of the intracellular C-terminal tail and therefore their expression cannot be detected using the commonly used antibody directed against epitopes of the C-terminal region. Detection of their expression is only possible using antibodies

Please cite this article in press as: Englezou PC et al. $P2X_7R$ activation drives distinct IL-1 responses in dendritic cells compared to macrophages. Cytokine (2015), http://dx.doi.org/10.1016/j.cyto.2015.05.013

directed against epitopes of the extracellular loop of the receptor, however, they can be distinguished from the full-length variants due to a difference in protein size (approximately 60 kDa), as shown by Masin and colleagues [29]. Nevertheless, it is clear that with the current tools available in murine tissue it is only possible to distinguish at the protein level between full-length and loss-of-function variants, such as the $P2X_7A$ and $P2X_713b$ but not between the $P2X_7A$ and $P2X_7K$. The idea that different splice variants help shape the function of the full-length $P2X_7A$ variants in different cell types is beginning to emerge, which requires a more collective effort to profile the expression of the various splice variants in different mammalian tissues.

As BMDC preparations were ~70% DC, $CD11c^+$ cells were specifically targeted by patch clamping for electrophysiology studies. These experiments extend previous observations of $P2X_7R$ expression by DC populations and provide for the first time functional evidence of receptor expression in $CD11c^+$ murine BMDC with pharmacology similar to that of the recombinant murine receptor expressed in HEK cells [30]. Differential patterns of IL-1 production and secretion were recorded for the two cell types. BMM were more sensitive with respect to the threshold concentration of LPS necessary for priming, whereas BMDC were more effective at IL-1 secretion, which was more robust and was sustained across a wider range of ATP concentrations. For both cell types LPS priming resulted in intracellular IL-1 expression but challenge with ATP was required for cytokine secretion.

Differential LPS-induced IL-1 production by DC and macrophages has been reported previously by He and colleagues [19]. BMDC were found to express higher levels of constitutive NLRP3 than macrophages, thereby providing for more rapid inflammasome activation and IL-1β processing. However, in those experiments a combination of apyrase and $P2X_7R$ KO mice were used to demonstrate that neither ATP nor $P2X_7R$ signalling were required for LPS-induced (24 h treatment) cytokine release in murine BMDC [19]. Given that a single relatively low dose of apyrase was also employed in those experiments, it could be argued that such was insufficient to ensure that the transient, successive waves of ATP typical of the receptor activation were effectively degraded. Furthermore, the recent identification of functional splice variants of $P2X_7R$ in $P2X_7R$ KO mice [22,29] suggests that such mice must be used in conjunction with specific $P2X_7R$ inhibitors in order to provide definitive information as to the relevance of the receptor. In contrast, the investigations reported herein have employed the potent and specific $P2X_7R$ inhibitor A-740003 [31] which was shown to effectively block the release of IL-1β from both murine BMDC and BMM. Indeed, this is the first study to demonstrate inhibition of IL-1β in murine BMDC using this drug. Given the reported specificity of A-740003 for the $P2X_7R$, these data provide indirect but convincing evidence that a functional $P2X_7R$ is expressed on both cell types and demonstrates the requirement of $P2X_7R$ signalling in IL-1β release from *in vitro* cultured DC and macrophages. The receptor is also important for human immune cell function, with studies in subjects with the loss-of-function Glu496Ala $P2X_7R$ polymorphism revealing a requirement for a functional $P2X_7R$ for effective IL-1β or IL-18 secretion by monocytes [32]. Further, the $P2X_7R$ and its role in IL-1β production has been shown to be critical for the sensitization phase of contact hypersensitivity [27].

The selective prozone effects of high dose ATP on BMM, whereby intracellular IL-1β expression was down-regulated without concomitant secretion, suggested that the intracellular cytokine content is actively targeted for degradation. Both lysosomal and proteosomal pathways have been shown to be involved in the regulation of IL-1β bioavailability by facilitating the degradation of IL-1β molecules or individual inflammasome components [33,34]. In addition, autophagy is apparently more strictly controlled in DC [35]. Suppression of autophagy and constitutive expression of higher levels of inflammasome components [19] could theoretically contribute to more vigorous IL-1β production by DC. A differential capacity to regulate the bioavailability of ATP and its metabolites may also play a role. For example, DC have been shown to possess strong adenosine deaminase activity at the cell surface to overcome the suppressive effects of adenosine which accumulates as a result of ATP degradation and signals through P1 receptors to counter-act pro-inflammatory processes [36,37]. These processes provide mechanisms whereby DC are kept in a state of readiness for initiating immune and inflammatory responses whereas macrophages are maintained in a more quiescent state with little or no production of pro-inflammatory agents.

BMDC and BMM also displayed differential secretion of IL-1α and IL-6 with relatively little production of these cytokines recorded for BMM under any conditions. Classically IL-1α secretion does not require inflammasome activation, despite being up-regulated by the same TLR ligands that induce IL-1β production. However, recent evidence suggests that IL-1α may also be released via the classic inflammasome-dependent secretory pathway of IL-1β [38–40]. In BMM, which exhibit an immunosuppressive profile, both isoforms of IL-1 could be specifically targeted by autophagosomes for destruction [35]. The general consensus is that IL-1α is secreted via passive diffusion from necrotic DC following injury [41]. However, consistent with the results of the study reported herein, Fettelschoss and colleagues demonstrated $P2X_7R$-mediated IL-1α release by murine BMDC [40]. Thus, LPS-primed/ATP-challenged BMDC derived from NLRP3 and $P2X_7R$ KO mice failed to release IL-1α, as well as IL-1β. Additionally, consistent with previous reports [42], murine LPS-primed BMM failed to synthesize detectable levels of IL-6 highlighting further the divergent responses of DC and macrophages with respect to cytokine production induced by the same bacterial ligands/danger signals. In BMDC, IL-6 expression and release was driven by LPS-, not -ATP, signalling and was $P2X_7R$-independent.

In order to provide a possible mechanistic basis for the differential LPS- and ATP-driven cytokine responses by DC and macrophages transcriptional levels of two $P2X_7R$ functional splice variants was examined. As such, this study represents the first demonstration of the expression of the gain-of-function $P2X_7K$ transcripts by murine BMDC and BMM. However, the functional differences observed between the two cell types could not be reconciled on the basis of constitutive, or LPS-induced, differential splice variant mRNA expression. It is possible that splice variant expression modulates $P2X_7R$ function at the level of translation and would not therefore be resolved using the current methods. At present, the topic of splice variants and their relative contribution to $P2X_7R$ function in primary tissues is still in its infancy, but once appropriate tools become available, analysis of the interactions of the variant receptors with the various adaptor, anchor or scaffolding proteins and the ability to form stable $P2X_7R$ trimers on the cell surface membrane may show cell specific patterns.

The impact of ATP on BMDC viability was somewhat surprising. Thus, challenge with 5 mM ATP induced a substantial drop in the viability of LPS-primed BMDC (assessed as a function of PI staining) whereas 10 mM ATP had little impact on cell viability. However, assessment of viability using trypan blue exclusion as the end point indicated that there was no significant drop in viability in the presence of 5 mM ATP. This is consistent with a recent study demonstrating that organic dyes such PI could in theory enter through the $P2X_7R$ channel itself which under sustained activation with mM levels of ATP results in pore formation [43]. Thus, the enhanced PI staining observed in BMDC could reflect an active $P2X_7R$ channel that allows PI entry. At higher levels of ATP (10 mM), it is assumed that BMDC have a mechanism in place to

Please cite this article in press as: Englezou PC et al. $P2X_7R$ activation drives distinct IL-1 responses in dendritic cells compared to macrophages. Cytokine (2015), http://dx.doi.org/10.1016/j.cyto.2015.05.013

prevent pore formation in response to excessive exposure to ATP, which would result in irreversible cell damage. The kinetics of pore formation and the level of permeabilization in murine BMDC and BMM were examined further. Although the density of receptor expression was not examined, these YO-PRO-1 uptake assays provide information as to the functional properties of the receptor in the two cell types [44]. Application of mM levels of ATP induced pore formation and dye uptake in both unprimed and LPS-primed BMDC and BMM, suggesting that dye uptake is an ATP-mediated effect and the result of $P2X_7R$ activation. The pattern of dye uptake by BMM was similar to that observed previously in a murine microglial cell line [45]. The rate of dye uptake in LPS-primed and ATP-challenged (1 mM) BMDC was faster and the fluorescence signal was greater than that observed in LPS-primed BMM. Also of note was the fact that LPS-primed DC and macrophages displayed opposing responses to increasing concentrations of ATP. Whereas in BMM the levels of dye uptake increased markedly at higher concentrations of ATP, the converse was observed with BMDC. Similar responses to BMDC were reported recently for primary astrocyte cultures whereby YO-PRO-1 dye uptake was reduced at higher concentrations of ATP in a dose-dependent manner [46]. It is widely accepted that prolonged ATP-induced pore formation results in the loss of cell viability. Thus, DC, being frequently exposed to excessive levels of ATP at sites of tissue injury are perhaps required to distinctly regulate pore formation as a protective mechanism.

The molecular platform that forms the $P2X_7R$ pore and whether this facilitates the release of IL-1 cytokines remains elusive and somewhat controversial. Several reports implicate pannexin-1 hemichannels as mediators of the pore in mouse peritoneal macrophages. Others provide evidence that excludes a role for pannexin-1 channels as the $P2X_7R$ pore in the same cells and demonstrate that the $P2X_7R$ channel itself holds the capacity to allow the passage of nanometer-sized particles, such as YO-PRO-1 molecules, in $P2X_7R$-transfected HEK-293 cells (reviewed by [47]). It is speculated that $P2X_7R$-driven pore-mediated cell permeabilization could be facilitated by a number of different channels including the pannexins that can be recruited to form the $P2X_7R$ pore and this will depend upon the specific cell type and/or the type of inflammatory signal. Perhaps during antigen presentation to T-cells, DC employ a more directly targeted approach, such as the release of IL-1β loaded microvesicles or exosomes to deploy a strong cytokine signal to a specific cell.

5. Conclusions

Despite the many reports focusing on $P2X_7R$ activation and IL-1β release, few have considered possible differences in $P2X_7R$-driven responses between different cell types. The results of these investigations demonstrate that DC and macrophages display divergent patterns of cytokine expression, particularly with respect to IL-1. ATP-mediated $P2X_7R$ activation offers an efficient platform for the processing and release of IL-1β although it may not play a central role for all types of inflammatory responses. It is becoming increasingly apparent that the $P2X_7R$ has distinct physicochemical properties that are species, but also cell, specific. Thus far, research has been directed disproportionately toward macrophages and although DC and macrophages share the same myeloid lineage and some overlapping functions, it is clear that DC display distinct cell-specific properties with respect to $P2X_7R$ function and the regulation of the release of pro-inflammatory cytokines such as IL-1β. Understanding the cell-specific regulation of such cytokines may pay dividends with respect to manipulating such responses in health and disease.

Acknowledgement

P.C. Englezou was funded through a Medical Research Council CASE studentship jointly with BASF.

References

[1] van de Veerdonk FL, Netea MG. New Insights in the immunobiology of IL-1 family members. Front Immunol 2013;4(167):1–11.
[2] Dinarello CA, Simon A, van der Meer JW. Treating inflammation by blocking interleukin-1 in a broad spectrum of diseases. Nat Rev Drug Discov 2012;11:633–52.
[3] Watters TM, Kenny EF, O'Neill LA. Structure, function and regulation of the Toll/IL-1 receptor adaptor proteins. Immunol Cell Biol 2007;85:411–9.
[4] Carta S, Lavieri R, Rubartelli A. Different members of the IL-1 family come out in different ways: DAMPs vs. cytokines? Front Immunol 2013;4(123):1–9.
[5] Dinarello CA. Immunological and inflammatory functions of the interleukin-1 family. Annu Rev Immuno 2009;27:519–50.
[6] Gross O. Measuring the inflammasome. Methods Mol Biol 2012;844:199–222.
[7] Rider P, Carmi Y, Guttman O, Braiman A, Cohen I, Voronov E, et al. IL-1alpha and IL-1beta recruit different myeloid cells and promote different stages of sterile inflammation. J Immunol 2011;187:4835–43.
[8] Eder C. Mechanisms of interleukin-1beta release. Immunobiology 2009;214:543–53.
[9] Watkins LR, Hansen MK, Nguyen KT, Lee JE, Maier SF. Dynamic regulation of the proinflammatory cytokine, interleukin-1beta: molecular biology for non-molecular biologists. Life Sci 1999;65:449–81.
[10] Franchi L, Munoz-Planillo R, Reimer T, Eigenbrod T, Nunez G. Inflammasomes as microbial sensors. Eur J Immunol 2010;40:611–5.
[11] Dinarello CA. Unraveling the NALP-3/IL-1beta inflammasome: a big lesson from a small mutation. Immunity 2004;20:243–4.
[12] Perregaux DG, McNiff P, Laliberte R, Conklyn M, Gabel CA. ATP acts as an agonist to promote stimulus-induced secretion of IL-1 beta and IL-18 in human blood. J Immunol 2000;165:4615–23.
[13] Gross O, Yazdi AS, Thomas CJ, Masin M, Heinz LX, Guarda G, et al. Inflammasome activators induce interleukin-1alpha secretion via distinct pathways with differential requirement for the protease function of caspase-1. Immunity 2012;36:388–400.
[14] Hogquist K. Surviving without a TCR. Trends Immunol 2001;22:476–7.
[15] Di Virgilio F. Liaisons dangereuses: P2X(7) and the inflammasome. Trends Pharmacol Sci 2007;28:465–72.
[16] Lee BH, Hwang DM, Palaniyar N, Grinstein S, Philpott DJ, Hu J. Activation of P2X(7) receptor by ATP plays an important role in regulating inflammatory responses during acute viral infection. PLoS ONE 2012;7:e35812.
[17] Kahlenberg JM, Dubyak GR. Mechanisms of caspase-1 activation by P2X7 receptor-mediated K+ release. Am J Physiol Cell Physiol 2004;286. C1100-C8.
[18] Wewers M, Sarkar A. P2X7 receptor and macrophage function. Puriner Signall 2009;5:189–95.
[19] He Y, Franchi L, Nunez G. TLR agonists stimulate Nlrp3-dependent IL-1beta production independently of the purinergic P2X7 receptor in dendritic cells and in vivo. J Immunol 2013;190:334–9.
[20] Lister MF, Sharkey J, Sawatzky DA, Hodgkiss JP, Davidson DJ, Rossi AG, et al. The role of the purinergic P2X7 receptor in inflammation. J Inflamm 2007;4(5):1–14.
[21] Kaczmarek-Hajek K, Lorinczi E, Hausmann R, Nicke A. Molecular and functional properties of P2X receptors-recent progress and persisting challenges. Purinergic Signal 2012;8:375–417.
[22] Nicke A, Kuan YH, Masin M, Rettinger J, Marquez-Klaka B, Bender O, et al. A functional P2X7 splice variant with an alternative transmembrane domain 1 escapes gene inactivation in P2X7 knock-out mice. J Biol Chem 2009;284:25813–22.
[23] Denlinger L, Fisette P, Sommer J. Cutting edge: the nucleotide receptor P2X7 contains multiple protein-and lipid-interaction motifs including a potential binding site for bacterial lipopolysaccharide. J Immunol 2001;167:1871–6.
[24] Dearman RJ, Cumberbatch M, Maxwell G, Basketter DA, Kimber I. Toll-like receptor ligand activation of murine bone marrow-derived dendritic cells. Immunology 2009;126:475–84.
[25] Holliday MR, Dearman RJ, Basketter DA, Kimber I. Stimulation by oxazolone of increased IL-6, but not IL-10, in the skin of mice. Toxicology 1996;106:237–42.
[26] Roger S, Pelegrin P, Surprenant A. Facilitation of P2X7 receptor currents and membrane blebbing via constitutive and dynamic calmodulin binding. J Neurosci 2008;28:6393–401.
[27] Weber FC, Esser PR, Müller T, Ganesan J, Pellegatti P, Simon MM, et al. Lack of the purinergic receptor P2X7 results in resistance to contact hypersensitivity. J Exp Med 2010;207:2609–19.
[28] Chessell I, Grahames C. Dynamics of P2X7 receptor pore dilation: pharmacological and functional consequences. Drug Develop Res 2001;53:60–5.
[29] Masin M, Young C, Lim K, Barnes SJ, Xu XJ, Marschall V, et al. Expression, assembly and function of novel C-terminal truncated variants of the mouse P2X7 receptor: re-evaluation of P2X7 knockouts. Br J Pharmacol 2012;165:978–93.

Please cite this article in press as: Englezou PC et al. $P2X_7R$ activation drives distinct IL-1 responses in dendritic cells compared to macrophages. Cytokine (2015), http://dx.doi.org/10.1016/j.cyto.2015.05.013

[30] Chessell IP, Simon J, Hibell AD, Michel AD, Barnard EA, Humphrey PP. Cloning and functional characterisation of the mouse P2X7 receptor. FEBS Lett 1998;439:26–30.
[31] Honore P, Donnelly-Roberts D, Namovic M, Hsieh G, Chang ZZ, Mikusa JP, et al. A-740003 [N-(1-{[(cyanoimino)(5-quinolinylamino) methyl] amino}-2, 2-dimethylpropyl)-2-(3,4-dimethoxyphenyl) acetamide], a novel and selective P2X7 receptor antagonist, dose-dependently reduces neuropathic pain in the rat. J Pharmac Exp Therapy 2006;319:1376–85.
[32] Sluyter R, Shemon AN, Wiley JS. Glu496 to Ala polymorphism in the P2X7 receptor impairs ATP-induced IL-1 beta release from human monocytes. J Immunol 2004;172:3399–405.
[33] Lee J, Kim HR, Quinley C, Kim J, Gonzalez-Navajas J, Xavier R, et al. Autophagy suppresses interleukin-1beta (IL-1beta) signaling by activation of p62 degradation via lysosomal and proteasomal pathways. J Biol Chem 2012;287:4033–40.
[34] Ainscough JS, Gerberick GF, Zahedi-Nejad M, Lopez-Castejon G, Brough D, Kimber I, et al. Dendritic cell IL-1alpha and IL-1beta are polyubiquitinated and degraded by the proteasome. J Biol Chem 2014.
[35] Harris J, Hartman M, Roche C, Zeng SG, O'Shea A, Sharp FA, et al. Autophagy controls IL-1beta secretion by targeting pro-IL-1beta for degradation. J Biol Chem 2011;286:9587–97.
[36] Bours MJ, Swennen EL, Di Virgilio F, Cronstein BN, Dagnelie PC. Adenosine 5′-triphosphate and adenosine as endogenous signaling molecules in immunity and inflammation. Pharmacol Ther 2006;112:358–404.
[37] Desrosiers MD, Cembrola KM, Fakir MJ, Stephens LA, Jama FM, Shameli A, et al. Adenosine deamination sustains dendritic cell activation in inflammation. J Immunol 2007;179:1884–92.
[38] Keller M, Ruegg A, Werner S, Beer HD. Active caspase-1 is a regulator of unconventional protein secretion. Cell 2008;132:818–31.
[39] Brody DT, Durum SK. Membrane IL-1: IL-1 alpha precursor binds to the plasma membrane via a lectin-like interaction. J Immunol 1989;143:1183–7.
[40] Fettelschoss A, Kistowska M, LeibundGut-Landmann S, Beer HD, Johansen P, Senti G, et al. Inflammasome activation and IL-1beta target IL-1alpha for secretion as opposed to surface expression. Proc Natl Acad Sci USA 2011;108:18055–60.
[41] Yazdi AS, Guarda G, Riteau N, Drexler SK, Tardivel A, Couillin I, et al. Nanoparticles activate the NLR pyrin domain containing 3 (Nlrp3) inflammasome and cause pulmonary inflammation through release of IL-1alpha and IL-1beta. Proc Natl Acad Sci USA 2010;107:19449–54.
[42] Eigenbrod T, Park JH, Harder J, Iwakura Y, Nunez G. Cutting edge: critical role for mesothelial cells in necrosis-induced inflammation through the recognition of IL-1 alpha released from dying cells. J Immunol 2008;181:8194–8.
[43] Browne LE, Compan V, Bragg L, North RA. P2X7 receptor channels allow direct permeation of nanometer-sized dyes. J Neurosci 2013;33:3557–66.
[44] North RA. Molecular physiology of P2X receptors. Physio Rev 2002;82:1013–67.
[45] Bianco F, Ceruti S, Colombo A, Fumagalli M, Ferrari D, Pizzirani C, et al. A role for P2X7 in microglial proliferation. J Neurochem 2006;99:745–58.
[46] Yamamoto M, Kamatsuka Y, Ohishi A, Nishida K, Nagasawa K. P2X7 receptors regulate engulfing activity of non-stimulated resting astrocytes. Biochem Biophys Res Commun 2013;439:90–5.
[47] Pelegrin P. Many ways to dilate the P2X7 receptor pore. Br J Pharmacol 2011;163:908–11.

Please cite this article in press as: Englezou PC et al. $P2X_7R$ activation drives distinct IL-1 responses in dendritic cells compared to macrophages. Cytokine (2015), http://dx.doi.org/10.1016/j.cyto.2015.05.013